



Energy distributions and yields of sputtered C₂ and C₃ clusters

E. Vietzke^{*}, A. Refke, V. Philipps, M. Hennes

Institut für Plasmaphysik, Forschungszentrum Jülich GmbH, Association Euratom-KFA, D-52425 Jülich, FRG

Abstract

The sputtering of carbon materials by energetic particles leads mainly to the emission of monoatomic carbon, but also to C₂ and C₃ clusters. Time-of-flight measurements were performed to determine the energy distributions of C₁, C₂ and C₃ sputtered from graphite during 5 keV Ne⁺ impact. All energy distributions are characterized by the Thompson distribution with a surface binding energy of 7.5 eV for C, 3.5 eV for C₂ and 0.8 eV for C₃. Using these distribution data the flux ratios of sputtered C₂ and C₃ to sputtered C can be determined to be 0.06 for C₂/C and 0.03 for C₃/C by 5 keV Ar⁺ impact, 0.05 for C₂/C and 0.02 for C₃/C by 5 keV Ne⁺ impact and 0.06 for C₂/C and 0.01 for C₃/C by 5 keV He⁺ impact, respectively. Thus, 11% of all sputtered carbon is emitted as C₂ and in the case of 5 keV Ar⁺ impact 9% as C₃.

Keywords: Physical erosion; Desorption; Low Z material; Carbon

1. Introduction

Carbon materials are the most extensively used materials for plasma-facing components in present-day fusion devices. For the understanding and modelling of the impurity content and impurity transport in the plasma boundary of fusion devices the impurity sources have to be known, i.e. the formation yields and the energy distributions of the released particles. The energy of the particles determines their penetration depth into the plasma. Up to now, only sputtered monoatomic carbon atoms are assumed in modelling the sputter erosion of carbon materials. The effect of cluster formation is only mentioned in one earlier paper [1] and no yields for the C₂ and C₃ formation are known. Furthermore, the energy distribution of sputtered clusters is important in identifying emission mechanism and — as shown below — is also necessary for the determination of the sputtering yield of the carbon clusters.

The energy distribution of sputtered atoms from graphite and amorphous carbon films have been determined during ion bombardment as well as in TEXTOR tokamak dis-

charges [2–4] which can be characterized by the Thompson distribution in its simplest case [5]:

$$F(E) \cdot dE \propto \frac{E \cdot dE}{(E + E_B)^3}, \quad (1)$$

where E_B is the surface binding energy. This distribution is developed according to the collision cascade theory and describes very well the emission of C atoms. The E_B data ranging from 7.4 to 7.6 eV have been obtained for sputtered C by ion bombardment [2–4].

The emission mechanism for sputtered clusters or molecules is much more complex than that of sputtered atoms. In principle, two simple ideas have been discussed, the gas phase recombination model and the direct emission mechanism. The first model assumes that each constituent atom of the cluster receives independently a momentum from a collision cascade and is sputtered individually and agglomerate to clusters after having left the surface if their momenta are sufficiently aligned and comparable in magnitude. Calculations show as a consequence of these restrictions for the dimer formation that the energy distribution above the maximum energy decays steeper than E^{-2} , namely E^{-5} for $E \gg E_B$ or $E \gg D$, where D is the dissociation energy (reviewed in [6]). Indeed, experimentally observed kinetic energy distribution of metal dimers

^{*} Corresponding author. Tel.: +49-2461 613 113; fax: +49-2461 612 660; e-mail: E.Vietzke@kfa-juelich.de.

confirm this trend with a high energy tail between E^{-3} and E^{-4} .

Modern molecular dynamics calculation for Ag_2 sputtering [7] agree very well with the experimental observation of a E^{-4} tail.

The other model, the direct emission mechanism, is best suited for a preformed molecule or cluster in which the molecule as a whole receive in a single collision a kinetic energy corresponding to an E^{-2} energy distribution of the recoils in the collision cascade [8]. As long as the vibrational energy between the atoms in such molecules is smaller than the dissociation energy and the surface binding energy, the molecule will be stable and moves as an entity from the surface into the vacuum if the momenta are in the right direction. Under these conditions, the collision cascade physics can be applied and it predicts an E^{-2} tail of the energy distribution [9]. This model has been applied for the kinetic analysis of molecules emitted during ion-assisted etching of silicon [8] and sputtered sulphur, having the emission of mainly S_2 (reviewed in [10]). Reported effective surface binding energies obtained from such spectra are in most cases lower than tabulated sublimation energies [11]. One reason is that the internal excitation can reduce the effective surface binding energy by up to a factor of two [12].

This paper deals with the energy distribution measurements of C and the clusters C_2 and C_3 sputtered from graphite. Such clusters are important components in the sublimation of graphite and other carbon materials. Above 2400 K, C_3 emission dominates that of C component in the sublimation. The sublimation energies for these three components are 7.5 eV for C, 8.2 eV for C_2 and 8.7 eV for C_3 [13]. The bond strength of C_2 is 6.3 eV and that of each of the both bonds in C_3 is 6.8 eV [14].

As in the case of metals the dissociation energies of the

carbon clusters are smaller than the bulk sublimation energies. Thus, the single collision mechanism should not be applicable to C_2 and C_3 emission. However, it is very questionable that these two parameters alone determine the cluster emission. The bond characteristics of the graphite structure is very different from metallic bonds and additionally, the ion-modified graphite may have different bulk properties to the normal graphite.

2. Experimental and data evaluation

The scheme of the experimental set-up is shown in Fig. 1. Details of determining the energy distribution of sputtered particles by time-of-flight (TOF) are described in a previous paper [2]. Briefly, pyrolytic graphite samples (Union Carbide) were bombarded by pulsed 5 keV Ne^+ ion beam of $5 \cdot 10^{18} \text{ Ne}^+/\text{m}^2 \text{ s}$ under an angle of 22.5° with respect to the normal. The normal direction of the sample is the C direction of the pyrolytic graphite. The ion beam pulse has a width of 10 μs in the C_1 and C_2 case and 50 μs for C_3 . The arrival time and length of the ion pulse were measured by secondary electrons from the target. The emitted particles at 45° to the ion beam direction are directly detected after a flight path length s of 16.3 cm by a differentially pumped line-of-sight quadrupole mass spectrometer (QMS). The signals were collected in a multichannel counting device (2 μs channel width) which directly records the total TOF spectra, that means the TOF of neutrals passing the flight path of 16.3 cm and the TOF of these particles after ionization passing the QMS.

It is very well known that the QMS technique has drawbacks in determination the energy of particles by TOF [15], especially the particle energy effect on the extraction efficiency from the ionizing region and the transmission of

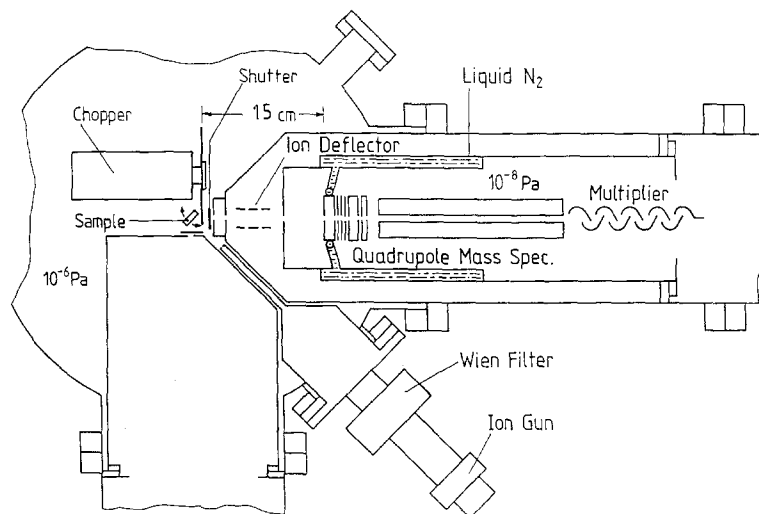


Fig. 1. Scheme of the experimental set-up.

the ionized particles. The used QMS was optimized to minimize this effect (ion energy of 75 eV with the disadvantage of a lower resolution, reduced entrance orifice, small ion spots etc.). The TOF of particles after ionization passing the QMS (t_D) was determined by a pulsed electron impact for the ionization. Within the resolution of these measurements there was no difference between thermal and sputtered particles ($t_D = 2.9M^{1/2}$, where M is the mass number). The transmission dependence on the mass of the incoming particles was determined by He, CH₄, Ne and Ar effusing from a Knudsen cell at 285 K in the target position to $T_{C_1}:T_{C_2}:T_{C_3} = 1.25:1:0.93$. The accuracy of the entire detection system was tested by measuring the energy distribution of sputtered silicon (Thompson distribution with $E_B = 5$ eV). The zero line of a TOF spectrum was obtained by averaging the noise at large TOFs.

The results obtained are presented in the form of TOF spectra of the neutrals passing the flight path length of 16.3 cm and are compared with the Thompson flux distribution $F(E)$ in its simplest case. As shown in Appendix A, the Thompson distribution results into the TOF signal function

$$S(t) \cdot dt \propto \frac{(t/t_0)^2 \cdot dt}{(1 + (t/t_0)^2)^3}, \quad (2)$$

where $t_0 = s/\alpha_0$ is the flight time of the most probable velocity $\alpha_0 = \sqrt{2 \cdot E_B/m}$. This distribution function has to be convoluted with the ion pulse width.

The ionization cross sections of the clusters C₂ and C₃ are not known [16]. For linear configurations (also C₃ is a linear molecule!) empirical rules are used in the mass spectroscopy:

$$\sigma_n = a * n * \sigma_1, \quad (3)$$

where n is the number of atoms in the cluster, σ_1 is the ionization cross sections of the carbon atom and a a constant between 0.5 and 1 [17]. We follow the assumption of [14] who is using $a = 0.7$ for C₂ and C₃. The cracking of the clusters by electron impact will be discussed in Section 3.

3. Results

Figs. 2–4 show the TOF spectra of C₁, C₂ and C₃ sputtered from graphite by a 5 keV Ne⁺ beam. As can be seen in the figures, all distributions can be reasonably fitted by Thompson distributions with a surface binding energies $E_B = 7.5$ eV for sputtered C₁, $E_B = 3.5$ eV for sputtered C₂ and $E_B = 0.8$ eV for sputtered C₃. The TOF spectrum of C₃ in Fig. 4 shows that the C₃ are emitted with significantly smaller energies than C₁ and C₂.

The accuracy in E_B data is estimated to be in the order of $\pm 15\%$, partly due to relatively small path length for the time-of-flight in comparison with flight time of the ionized

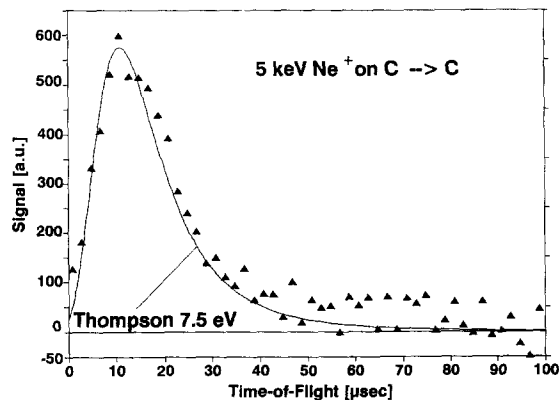


Fig. 2. Time-of-flight (TOF) spectrum of C₁ sputtered from graphite at room temperature during 5 keV Ne⁺ bombardment. Solid line: fitted Thompson distribution with a surface binding energy of 7.5 eV.

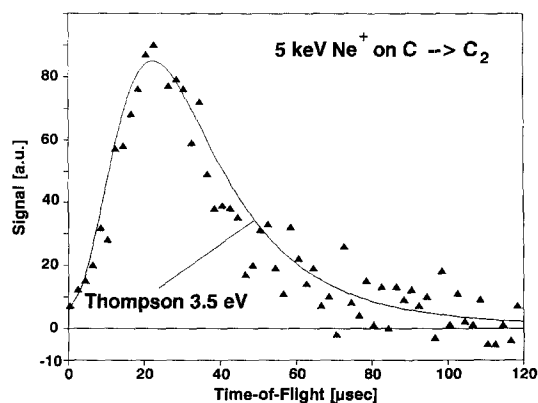


Fig. 3. Time-of-flight (TOF) spectrum of C₂ sputtered from graphite at room temperature during 5 keV Ne⁺ bombardment. Solid line: fitted Thompson distribution with a surface binding energy of 3.5 eV.

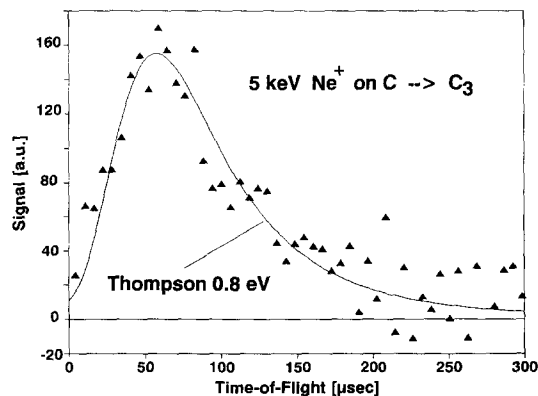


Fig. 4. Time-of-flight (TOF) spectrum of C₃ sputtered from graphite at room temperature during 5 keV Ne⁺ bombardment. Solid line: fitted Thompson distribution with an effective surface binding energy of 0.8 eV.

particles in the QMS, and to the instability of the ion spot at the target position. However, the resolution is sufficient for the main goal of these experiments to determine the ratios of the erosion fluxes for the C, C₂ and C₃ and also to determine the peak energy of the energy spectrum of sputtered atoms.

Similar TOF spectra are observed for 5 keV Ar⁺ impact. There was also no difference observable by using a continuous ion beam and chopping the emitted particles by a motor driven disk shown in Fig. 1.

No large effect on cracking of C₂ and C₃ by 50 eV electrons leading to C⁺ can be seen in the TOF spectrum of C. The hump above 20 eV and the scatter of the data above 50 eV is used to determine an upper limit of 20% for the cracking of C₂ and C₃ leading to C⁺.

The signal intensity ratios of total sputtered particles are observed to be 0.14 for S_{C₂}/S_{C₁} and 0.24 for S_{C₃}/S_{C₁} by 5 keV Ar⁺ impact, 0.12 for S_{C₂}/S_{C₁} and 0.14 for S_{C₃}/S_{C₁} by 5 keV Ne⁺ impact and 0.14 for S_{C₂}/S_{C₁} and 0.07 for S_{C₃}/S_{C₁} by 5 keV He⁺ impact, respectively.

The obtained energy distributions, the determined mass transmission dependence and the signal intensity ratios of total sputtered particles allow to determine the ratios of sputtering yields by $Y_{C_x}/Y_{C_1} = S_{C_x}/S_{C_1} * \sigma_1/\sigma_x * T_1/T_x * (E_{B,x}/E_{1,x} * M_1/M_x)^{1/2}$ to

$$Y_{C_2}/Y_{C_1} = 0.056, \quad Y_{C_3}/Y_{C_1} = 0.030$$

for 5 keV Ar⁺ impact,

$$Y_{C_2}/Y_{C_1} = 0.054, \quad Y_{C_3}/Y_{C_1} = 0.016$$

for 5 keV Ne⁺ impact and

$$Y_{C_2}/Y_{C_1} = 0.058, \quad Y_{C_3}/Y_{C_1} = 0.008$$

for 5 keV He⁺ impact,

i.e. in all three cases 10% of total sputtered carbon is emitted as C₂ and in the case of argon ion impact 8% as C₃. The accuracy of these ratios is estimated to be only within a factor of two due to the uncertainties in the ionization cross section and the scatter in the data of the transmission between that of CH₄ and Ne.

4. Discussion

The main goal of this investigation was the determination of the relative sputtering yield of C, C₂ and C₃. In the investigated mass range, the yield ratio Y_{C₂}/Y_{C₁} is independent on the mass of the impinging ion whereas the yield ratio Y_{C₃}/Y_{C₁} is increasing with increasing ion mass. Possible reasons for the mass dependence of Y_{C₃}/Y_{C₁} are the depth of the implantation or the higher density of the defects and interstitials in the collision cascade by implanting a heavier ion. The last-mentioned reason would suggest that C₃ is formed in a reaction of C and C₂. If the ratio Y_{C₃}/Y_{C₁} depends on the implantation depth it would also depend on the energy of the impinging ion, i.e. it

would be much larger in fusion plasmas. The energy dependence of the sputtering ratio Y_{C₃}/Y_{C₁} was not investigated in detail. However, one experiment with 3 keV Ar⁺ did not support any energy dependence.

As already mentioned in the introduction the emission mechanisms of sputtered clusters are complex and the following discussion can only touch the problems rather than present a final model for the cluster emission.

The surface binding energy of 7.5 eV from the fitted Thompson distribution for C₁ agrees very well with earlier measurements and is in excellent agreement with the value of the sublimation energy of an unirradiated solid, i.e. such a result is expected from the collision cascade sputtering theory. Surprisingly, the modification of the graphite by ion bombardment [18,19] does not seem to change the bond characteristics for the carbon atom emission.

The observed TOF spectrum for the sputtered C₂ cluster may still be in line with models of a collision cascade driven formation of dimers, even the determined fitting parameter E_B has a value of only 40% of the sublimation energy from an unirradiated solid. In the literature, it is discussed that the surface binding force acts in a more complex manner on dimers with several more degrees of freedom than for atomic particles with the result that the effective binding energy determined from the energy distribution is mostly smaller than the measured sublimation energy [12]. On the other hand, the surface binding energy for C₂ from a modified structure due to ion bombardment is not known and can also not be measured by thermal sublimation due to annealing effects (graphitization) with increasing temperature.

New and a surprising result is the energy distribution of C₃ cluster fitted by a Thompson distribution with an E_B = 0.8 eV. This value is far below the sublimation energy of 8 eV of an unirradiated solid and can not be explained by single-collision emission mechanism from a preformed bound state. As mentioned above, the dependence of the yield ratio Y_{C₃}/Y_{C₁} on the mass of the impinging ion suggests an C₃ formation in a reaction of C and C₂. This assumption is supported by the relatively low effective surface binding energy E_B which is characteristic for molecular reactions. Such low effective surface binding energy is observed in the chemical sputter reaction of O⁺ with graphite leading to CO with an E_B = 0.28 eV [20]. For the CO formation, a two step mechanism was assumed. CO is formed at the implantation depth [21], once adsorbed (induced by ion bombardment?) in the near surface region and sputtered from this adsorbed state by a single collision with a recoil particle of the collision cascade. The energy distribution of CO shows an E⁻² tail at energies above the maximum which is characteristic for a single collision event. This rather complicated procedure was mainly assumed in the previous paper due to the fact that the CO is bonded with 2.5 eV in an O⁺ irradiated graphite as determined by thermal desorption, roughly ten times larger than E_B from the energy distribution.

If such a complicated mechanism also occurs for the C_3 emission, E_B may only be interpreted by molecular dynamics calculations similar to ones in [7]. Such a model calculation could also possibly explain the contradiction that the value of $E_B = 0.8$ eV is larger than the adsorption energy of a physisorbed C_3 on unmodified graphite which has been determined to be smaller than 0.15 eV [22].

It has been observed that direct fragmentation of sputtered large clusters occurs after the ejection due to high internal energy from the collisional formation process [23]. If a main contribution of the above shown C , C_2 , C_3 TOF spectra would have its origin in fragmentation from larger clusters two peaks should appear at TOFs corresponding to the velocity $v = v_{\text{cluster}} \pm (2E_{\text{cm}}/m)^{1/2}$, where v_{cluster} is the velocity of the cluster before fragmentation and E_{cm} is the energy in the center of mass of the emitted atom. Since such a second peak is not observed up to times of 1 ms we can exclude a contribution from fragmentation in the TOF spectra in Figs. 2–4.

5. Conclusions

From the measured energy distributions and the signal intensities of sputtered C , C_2 and C_3 species under 5 keV He^+ , Ne^+ and Ar^+ bombardment of graphite the ratios of sputtering yields have been determined to be $Y_{C_2}/Y_{C_1} \approx 0.06$ and Y_{C_3}/Y_{C_1} between 0.01 and 0.03 increasing with increasing mass of impact ions.

The energy distribution for C_2 clusters with an effective surface binding energy of 3.5 eV (40% of the sublimation energy) and the E^{-2} high energy tail suggests a direct emission mechanism of preformed clusters. The dependence of the yield ratio Y_{C_3}/Y_{C_1} on the mass of the impinging ion, the very low effective surface binding energy for sputtered C_3 and the E^{-2} high energy tail in the energy distribution suggest a molecular reaction mechanism under ion bombardment, i.e. C_3 is formed in a reaction of a mobile carbon atom with the damaged carbon structure and once adsorbed in the near surface region sputtered from this adsorbed state in a single collision event with a recoil of the collision cascade.

Molecular dynamics calculation may yield a better understanding of the cluster emission mechanisms and can explain whether such observed effective surface binding energies are in agreement with the proposed models of carbon cluster emission.

Appendix A. Transformation of a flux distribution into a time dependent signal distribution

In this paper the Thompson flux distribution (Eq. (1)) is used

$$F(E) \cdot dE \propto \frac{E}{(E + E_B)} \cdot dE. \quad (\text{A.1})$$

This distribution has to be transformed into a time-dependent signal function $S(t)$ by using the following relations: flight time $t = s/v$, where s is the flight path and v the velocity, and $E = \frac{1}{2}mv^2 = (m \cdot s^2)/(2 \cdot t^2)$ results into $dE/dt = -m \cdot s^2/t^3$, $t_0 = s/\alpha_0$ is the flight time of the normalized velocity $\alpha_0 = \sqrt{2 \cdot E_B/m}$. Note: The signal is proportional to the density $n(t) \propto \text{flux}/\text{velocity} \propto t$, i.e. the distribution has to be multiplied by t resulting into:

$$S(t) \cdot dt \propto F(E(t)) \cdot t \frac{dE}{dt} dt \propto (t/t_0)^2 \cdot dt / (1 + (t/t_0)^2)^3 \quad (\text{A.2})$$

whereby $E/(E + E_B)$ as function of t is transformed into $f(t) \propto (t/t_0)^4 \cdot dt/(1 + (t/t_0)^2)^3$. Finally, the TOF signal distribution reads by using time units to, i.e. $T = t/t_0$

$$S(T) \cdot dT \propto \frac{T^2 \cdot dT}{(1 + T^2)^3}. \quad (\text{A.3})$$

This distribution has to be convoluted with the ion pulse width from $-T_p/2$ to $T_p/2$

$$S^*(T) \cdot dT \propto dT \cdot \int_{-T_p/2}^{T_p/2} \frac{(T - T')^2 \cdot dT'}{(1 + (T - T')^2)^3} \quad (\text{A.4})$$

by substituting $x = T - T'$, Eq. (A.4) results for times above $T_p/2$ into

$$S^*(T) \cdot dT \propto -dT \int_{T+T_p/2}^{T-T_p/2} \frac{x^2 \cdot dx}{(1 + x^2)^3} = \frac{dT}{8} \cdot \left(\frac{x^3 - x}{(1 + x^2)^2} + \arctan x \right) \Bigg|_{T-T_p/2}^{T+T_p/2} \quad (\text{A.5})$$

For times below $T_p/2$ the upper limit of the integral would be zero instead of $T - T_p/2$.

References

- [1] V. Philipps, K. Flaskamp and E. Vietzke, J. Nucl. Mater. 111–112 (1982) 781.
- [2] E. Vietzke, K. Flaskamp, M. Hennes et al., Nucl. Instr. Methods B 2 (1984) 617.
- [3] E. Pasch, P. Bogen and Ph. Mertens, J. Nucl. Mater. 196–198 (1992) 1065.
- [4] P. Bogen and D. Rusbüldt, J. Nucl. Mater. 196–198 (1992) 179.
- [5] M.W. Thompson, Philos. Mag. 18 (1968) 377.
- [6] H.M. Urbassek and W.O. Hofer, Mat. Fys. Medd. 43 (1993) 97.
- [7] A. Wucher and B.J. Garrison, Surf. Sci. 260 (1992) 257.
- [8] R.A. Haring, H.E. Roosendaal and P.C. Zalm, Nucl. Instr. Methods B 28 (1987) 205.

- [9] P. Sigmund, in: *Sputtering by particle bombardment I*, ed. R. Behrisch (Springer, Berlin, 1981) p. 9.
- [10] R. de Jonge, J. Los and A.E. de Vries, *Nucl. Instr. Methods B* 30 (1988) 159.
- [11] R.A. Haring, R. Pedrys, D.J. Oostra et al., *Nucl. Instr. Methods B* 5 (1984) 476.
- [12] H.M. Urbassek, *J. Phys. Condens. Matter* 4 (1992) 4871.
- [13] H.B. Palmer and M. Shalef, in: ed. P.L. Walker, *Chem. Phys. Carbon* 4 (1968) 85.
- [14] K.A. Gingerich et al., *J. Am. Chem. Soc.* 116 (1994) 3884.
- [15] R. Braun and P. Hess, *Int. J. Mass Spectrom. Ion Processes* 125 (1993) 229.
- [16] W. Hastic et al., *High Temp. High Pressures* 20 (1988) 73.
- [17] J. Drowart, in: ed. J. Marsel, *Proc. Int. School Mass Spectr., Ljubljana* (1971) p. 187.
- [18] E. Vietzke and V. Philipps, *Nucl. Instr. Methods B* 23 (1987) 449.
- [19] E. Vietzke, V. Philipps and K. Flaskamp, *J. Nucl. Mater.* 162–164 (1989) 898.
- [20] E. Vietzke, A. Refke, V. Philipps et al., *J. Nucl. Mater.* 220–222 (1995) 249.
- [21] A. Refke, V. Philipps and E. Vietzke, *J. Nucl. Mater.* 212–215 (1994) 1255.
- [22] V. Philipps, E. Vietzke and K. Flaskamp, *Surf. Sci.* 178 (1986) 806.
- [23] W. Begemann, K.H. Meiwes-Broer and H.O. Lutz, *Phys. Rev. Lett.* 56 (1986) 2248.